

# A Model for a Thermally Induced Polymer Coil-to-Globule Transition

David S. Simmons and Isaac C. Sanchez\*

Department of Chemical Engineering, The University of Texas at Austin, 1 University Station C0400, Austin, Texas 78712-0231

Received January 22, 2008; Revised Manuscript Received May 28, 2008

**ABSTRACT:** A semiquantitative mean-field model for the thermally induced (heating-induced) polymer coil-to-globule transition (HCGT) is developed with no adjustable parameters. The transition temperature  $\Theta$  is given for a long chain by the equation  $\Theta = 2T_p^*[1 - \bar{\rho}^B(\Theta)]$ , where  $T_p^*$  is the characteristic temperature of the polymer and  $\bar{\rho}^B(\Theta)$  is the bulk solvent density at the transition temperature. The variables  $\bar{\rho}^B$  and  $T_p^*$  are obtained by invoking the Sanchez–Lacombe (S–L) equation of state. Calculated HCGT temperatures show good agreement with experimental lower critical solution temperatures (LCSTs). The predicted globular state is characterized by the dominance of attractive polymer self-interactions over excluded volume interactions. There is a critical value of the ratio of polymer to solvent S–L characteristic temperature below which no HCGT transition is predicted for an infinite chain. This model can be easily generalized to treat cross-linked gels and their contraction–expansion characteristics.

## Introduction

Coil–globule transitions have long been considered relevant in diverse settings ranging from synthetic polymer applications to the functionality of biopolymers such as DNA and proteins. Possibly as a result of its relative tractability, the focus of theory,<sup>1–5</sup> experiment,<sup>6–14</sup> and simulation<sup>15,16</sup> has been a reversible cooling-induced coil-to-globule transition (CCGT) that is well-known to be associated with the system upper critical solution temperature (UCST). In 1979, Sanchez proposed that a reversible thermally induced (heating induced) coil-to-globule transition (HCGT) should be associated with the lower critical solution temperature (LCST) transition.<sup>1</sup> Computer simulation has supported the existence of this “inverse” transition,<sup>17–22</sup> and further studies have suggested that it may be the dominant mechanism in many applications. In order to facilitate understanding and application of this mechanism, this paper outlines a theoretical model for the HCGT transition.

The HCGT is of particular interest due to its connection with the functionality of biological macromolecules. Early studies indicated that coil–globule transitions are of relevance in the functionality of DNA.<sup>23,24</sup> More recent studies have confirmed the presence of a coil–globule transition in DNA<sup>25–27</sup> and have shown a relationship between protein coil–globule transitions and folding.<sup>28–31</sup> Urry reports that the LCST “transition provides a fundamental mechanism whereby proteins fold and function and whereby the energy conversions that sustain living organisms can occur at constant temperature.”<sup>32</sup> Since biomolecules often function at low concentrations, it is likely that this transition is better described as a HCGT than an LCST.

The HCGT has also become a subject of interest due to its role in the behavior of so-called “stimuli responsive” or “smart” polymers. These materials typically exhibit a reversible swelling transition with changes in environmental conditions such as temperature, pH, or salinity. At low concentrations, this transition may take the form of a CGT. For example, poly(*N*-isopropylacrylamide) (PNIPA) has been heavily studied for use in biological systems due to the fact that it exhibits an LCST/HCGT near physiological conditions.<sup>33–37</sup> These systems are of particular interest for use in controlled drug delivery due to their ability to release an absorbed drug in response to physiological triggers.

Recently, a limited model for an HCGT has been developed for the case of a symmetric solvent—one in which the solvent–polymer interaction, the polymer self-interaction, and the solvent self-interaction are all equal.<sup>38</sup> However, to our knowledge, no general model exists that predicts HCGT temperature and behavior for arbitrary combinations of polymer and solvent. The semiquantitative model for the HCGT presented here is based upon Sanchez’ 1979 model<sup>1</sup> for the CCGT of a polymer in vacuum. It extends the former approach by considering the insertion of a polymer chain into a solvent of finite density. This leads to calculations of the CGT temperature and of the equilibrium gyration radius as a function of temperature. For the purpose of numerical results, bulk solvent density is obtained via the Sanchez–Lacombe (S–L) model,<sup>39</sup> but in principle any equation of state or empirical correlation could be used.

## Theory

**A. Model Description.** Consider a single polymer chain in an infinite solvent on a lattice of coordination number  $z$ . The chain consists of a random walk of  $r$  units, proportional to molecular weight, connected by  $r - 1$  steps with  $z$  possible directions to be taken at each step. Such a polymer will pervade a volume  $V$  that will scale as the cube of the chain radius of gyration  $S$ . The bulk solvent far from the chain will be unaffected by the presence of the chain and will exhibit a constant chemical potential with respect to any property of the chain. The solvent within the chain pervaded volume will be in equilibrium with the bulk solvent and will satisfy equality of chemical potential with the bulk solvent. The chain itself will occupy an average volume fraction  $\phi$  within its pervaded volume, given by

$$\phi \sim \frac{r\sigma^3}{S^3} \quad (1)$$

where  $\sigma^3$  is the volume of one monomer unit.

The gyration radius of the chain may be related to that of an ideal chain via the expansion factor  $\alpha^2$ , defined as

$$\alpha^2 \equiv S^2/\langle S^2 \rangle_0 \quad (2)$$

where  $\langle S^2 \rangle_0$  is the unperturbed average value of  $S^2$ . For an ideal random walk,  $\langle S^2 \rangle_0 \sim r\sigma^2$ . Substitution of eq 2 into eq 1 yields a relationship between the expansion factor and mer density:

\* To whom correspondence should be addressed.

$$\alpha^2 = \frac{a}{r^{1/3} \phi^{2/3}} \quad (3)$$

where  $a$  is some dimensionless constant.

At any given temperature and pressure the chain will exhibit a mean-square gyration radius  $\langle S^2 \rangle$  corresponding to a mean expansion factor  $\langle \alpha^2 \rangle$ , defined as

$$\langle \alpha^2 \rangle \equiv \langle S^2 \rangle / \langle S^2 \rangle_0 \quad (4)$$

For values of the mean expansion factor significantly less than unity, the chain is much more collapsed than the ideal state and is expected to behave as a globule with gyration radius scaling  $\langle S^2 \rangle \sim r^{2/3}$ . For values significantly greater than unity, the chain is much more expanded than the ideal state and is expected to behave as an expanded coil with scaling  $\langle S^2 \rangle \sim r^{6/5}$ . It is therefore appropriate to define the coil globule transition by the criterion

$$\langle \alpha^2 \rangle_{\text{CGT}} = 1 \quad (5)$$

at which point the chain is in its ideal state such that  $\langle S^2 \rangle \sim r$ . Furthermore, the type of CGT may be established by noting that  $\partial \langle \alpha^2 \rangle / \partial T > 0$  at a CCGT and  $\partial \langle \alpha^2 \rangle / \partial T < 0$  at an HCGT.

**B. Calculation of the CGT.** The partition function for the chain as a function of  $S$  may be written in terms of the chain insertion parameter  $\mathbf{B}$  as

$$\Omega(S) \sim P_0(S) \mathbf{B} \quad (6)$$

where  $P_0(S)$  is the distribution of radii of gyration for an ideal chain. Because the chemical potential of the solvent is a constant with respect to all chain properties, only the partition function of the chain need be considered in determining the equilibrium radius of gyration. Given  $\mathbf{B}$  and  $P_0(S)$ , the mean-square radius of gyration as a function of temperature and pressure may be rigorously determined by an average:

$$\langle S^2 \rangle = \frac{\int S^2 \Omega \, d\phi}{\int \Omega \, d\phi} \quad (7)$$

Since  $SP_0(S)$  has a maximum at  $S^2 = \langle S^2 \rangle$ , an excellent approximation for the mean-square radius of gyration is<sup>1</sup>

$$\left. \frac{\partial \ln(S\Omega)}{\partial S} \right|_{S^2=\langle S^2 \rangle} = 0 \quad (8)$$

which provides a simpler calculation than eq 7. The chain radius of gyration must satisfy eq 8 at all temperatures. As noted by eq 5, a chain at the CGT must additionally correspond to the ideal gyration radius. Thus, for the CGT

$$\left. \frac{\partial \ln(S\Omega)}{\partial S} \right|_{S^2=\langle S^2 \rangle, \alpha=1} = \left. \frac{\partial \ln \mathbf{B}}{\partial S} \right|_{S^2=\langle S^2 \rangle, \alpha=1} = 0 \quad (9)$$

where use has been made of

$$\left. \frac{\partial \ln[SP_0(S)]}{\partial S} \right|_{S^2=\langle S^2 \rangle, \alpha=1} = 0 \quad (10)$$

This demonstrates that the CGT is completely determined by thermodynamics and is independent of the ideal gyration radius distribution,  $P_0(S)$ .

Within a mean-field approximation the insertion factor is given by

$$\mathbf{B} = \mathbf{P} \exp[-\beta \langle \psi \rangle] \quad (11)$$

where  $\langle \psi \rangle$  is the average interaction of the chain with itself and with the solvent,  $\beta = 1/kT$ , and  $\mathbf{P}$  is the mean-field hard-core probability of successfully inserting the chain into a solvent of reduced density  $\tilde{\rho}^B$  in the bulk.

The reduced solvent density  $\tilde{\rho}$  within the pervaded volume may differ from  $\tilde{\rho}^B$ , yielding an insertion probability of

$$\mathbf{P} = \prod_{j=0}^{r-1} \left( 1 - \tilde{\rho} - \frac{j}{r} \phi \right) \quad (12)$$

where  $\tilde{\rho}$  is the occupied volume fraction of the solvent within the pervaded volume of the chain. The factor  $1 - \tilde{\rho} - j\phi/r$  equals the fraction of unoccupied sites when the  $j$ th-mer is introduced into the solvent. With Sterling's approximation eq 12 becomes

$$\mathbf{P} \cong e^{-r} \frac{(1 - \tilde{\rho})^{\frac{1-\tilde{\rho}}{\phi} r}}{(1 - \tilde{\rho} - \phi)^{\frac{1-\tilde{\rho}-\phi}{\phi} r}} \quad (13)$$

Although the same result may be arrived at via a lattice-free approach, the mean-field interaction energy is calculated as if the chain was on a lattice of coordination number  $z$ :

$$\langle \psi \rangle = -z \left[ r \varepsilon_{\text{sp}} \tilde{\rho} + \sum_{j=1}^{r-1} \frac{j}{r} \phi \varepsilon_{\text{pp}} \right] \quad (14)$$

Here  $\varepsilon_{\text{pp}}$  and  $\varepsilon_{\text{sp}}$  are the polymer self-interaction energy and polymer-solvent interaction energies, respectively. For large  $r$  eq 14 becomes

$$\langle \psi \rangle = -r(\varepsilon_{\text{pp}}^* \phi + 2\varepsilon_{\text{sp}}^* \tilde{\rho}) \quad (15)$$

where

$$\varepsilon_{ij}^* = \frac{z \varepsilon_{ij}}{2} \quad (16)$$

Equation 11 now becomes

$$\mathbf{B} = e^{-r} \frac{(1 - \tilde{\rho})^{r(1-\tilde{\rho})\phi/r}}{(1 - \tilde{\rho} - \phi)^{r(1-\tilde{\rho}-\phi)/\phi/r}} \exp[\beta r(\varepsilon_{\text{pp}}^* \phi + 2\varepsilon_{\text{sp}}^* \tilde{\rho})] \quad (17)$$

Substituting eq 17 into eq 9 for the CGT yields

$$\frac{\varepsilon_{\text{pp}}^*}{k\Theta} \langle \phi \rangle_0 + [\ln(1 - \varphi_0) + \varphi_0]/\varphi_0 = 0 \quad (18)$$

where  $\langle \phi \rangle$  is the mean occupied volume fraction of the chain in the pervaded volume,  $\Theta$  is the CGT temperature, "0" subscripts denote values at the transition (where  $\langle \alpha^2 \rangle = 1$ ), and

$$\varphi \equiv \frac{\langle \phi \rangle}{1 - \tilde{\rho}} < 1 \quad (19)$$

Expanding the logarithmic term in eq 18 gives

$$\frac{T_p^*}{\Theta} \langle \phi \rangle_0 - \left[ \frac{\varphi_0}{2} + \frac{\varphi_0^2}{3} + \dots \right] = \langle \phi \rangle_0 \left[ \frac{T_p^*}{\Theta} - \frac{1}{2(1 - \tilde{\rho})} - \frac{\langle \phi \rangle_0}{3(1 - \tilde{\rho})^2} - \dots \right] = 0 \quad (20)$$

where  $T_p^* = \varepsilon_{\text{pp}}^*/k$  is a characteristic temperature of the polymer. In the limit of infinite molecular weight,  $r \rightarrow \infty$ ,  $\langle \phi \rangle_0 \rightarrow 0$ ,  $\tilde{\rho} \rightarrow \tilde{\rho}^B$ , and from eq 20, the coil-globule transition temperature is given by the simple equation:

$$\Theta = 2T_p^*[1 - \tilde{\rho}^B(\Theta)] \quad (21)$$

Furthermore, the first order correction  $\delta\Theta$  to this transition temperature for a chain of finite length is obtained from eq 20 and yields

$$\frac{|\delta\Theta|}{T_p^*} = \frac{4}{3} \phi_0 \sim r^{-1/2} \quad (22)$$

where  $\delta\Theta = \Theta(r) - \Theta(\infty)$ .

**C. Solvent Density in the Chain Pervaded Volume.** For the case of finite chain length  $\bar{\rho} \neq \bar{\rho}^B$ , and evaluation of eq 18 requires an expression relating these two variables. Invoking equality of chemical potentials near and far from the chain yields such a relation. Chemical potential is calculated via the insertion parameter

$$\mu_s = kT \ln \left( \frac{\rho \lambda^3}{B_s} \right) \quad (23)$$

where  $B_s$  is the insertion parameter of a solvent molecule,  $\rho$  is the solvent number density, and  $\lambda$  is the familiar thermal wavelength,  $h/(2\pi mkT)^{1/2}$ . Equating eq 23 in the pervaded volume and in the bulk gives

$$\bar{\rho} = \bar{\rho}^B \frac{B_s}{B_s^B} \quad (24)$$

where variables without superscripts denote values within the chain pervaded volume and values with superscript B denote values in the bulk. The insertion factor is given by eq 11 as before. For the solvent in the pervaded volume this yields

$$B_s = (1 - \langle \phi \rangle - \bar{\rho})^{r_s} \exp[\beta r_s (\varepsilon_{ss}^* \bar{\rho} + 2\varepsilon_{sp}^* \langle \phi \rangle)] \quad (25)$$

where  $\varepsilon_{ss}^*$  is as shown in eq 16 for the solvent–solvent interaction energy and  $r_s$  is the number of lattice sites occupied by the solvent molecule. The insertion factor for the bulk solvent is

$$B_s^B = (1 - \bar{\rho}^B)^{r_s} \exp[\beta r_s \varepsilon_{ss}^* \bar{\rho}^B] \quad (26)$$

Combining eq 26 and eq 25 with eq 24 yields

$$\bar{\rho} = \bar{\rho}^B \left( \frac{1 - \langle \phi \rangle - \bar{\rho}}{1 - \bar{\rho}^B} \right)^{r_s} \exp[\beta r_s (\varepsilon_{ss}^* (\bar{\rho} - \bar{\rho}^B) + 2\varepsilon_{sp}^* \langle \phi \rangle)] \quad (27)$$

**D. Gyration Radius of the Chain.** Calculating the radius of gyration via eq 8 at an arbitrary temperature other than the CGT requires an explicit expression for the ideal gyration radius distribution  $P_0(S)$ . This may be well approximated through the first four even moments by<sup>40</sup>

$$P_0(S) dS \sim S^6 \exp\left(-\frac{7}{2} \frac{S^2}{\langle S^2 \rangle_0}\right) = S^6 \exp\left(-\frac{7}{2} \frac{a}{r^{1/3} \phi^{2/3}}\right) \quad (28)$$

Applying eq 28 with eq 8 and eq 6 yields the following equation for the chain occupied volume fraction:

$$\frac{7}{3}(\langle \alpha^2 \rangle - 1) = -r\{\beta \varepsilon_{pp}^* \langle \phi \rangle + [\ln(1 - \varphi) + \varphi/\varphi]\} \quad (29)$$

In the limit of long chain length, the CGT will be given to a good approximation by eq 21, allowing eq 29 to be rewritten as

$$\frac{7}{3}(\langle \alpha^2 \rangle - 1) = -r\left\{\frac{\Theta}{T} \varphi + [\ln(1 - \varphi) + \varphi/\varphi]\right\} \quad (30)$$

Equation 30 is identical in functional form to what was obtained for a chain in a vacuum ( $\bar{\rho} = 0$ ).<sup>1</sup>

## Results and Discussion

Relating these equations to experiment is greatly aided by making the identification that  $T_p^*$  in eq 21 is equivalent to the S–L temperature parameter for the polymer. Likewise, all  $\varepsilon_{ii}^*$  may be obtained by noting that within the S–L theory  $T_i^* = \varepsilon_{ii}^*/k$ . The cross-interaction term may be approximated by a geometric average. The bulk solvent density  $\bar{\rho}^B$  as a function of temperature required by eqs 21 and 27 may be obtained by any number of experimental or theoretical approaches. In the present study it is determined via the S–L equation of state for the bulk solvent:

$$(\bar{\rho}^B)^2 + \tilde{P} + \tilde{T}[\ln(1 - \bar{\rho}^B) + (1 - 1/r_s)\bar{\rho}^B] = 0 \quad (31)$$

where  $\tilde{T}$  and  $\tilde{P}$  are the reduced temperature and pressure and  $r_s$  is the S–L length parameter of the solvent. The appropriate equation of state parameters ( $T_s^*$ ,  $P_s^*$ ,  $r_s$ ) for many solvents have been tabulated.<sup>41</sup> The reduced solvent density  $\bar{\rho}^B$  is also related to equation of state parameters by

$$\bar{\rho}^B = \rho/\rho^* \quad \text{with} \quad \rho^* = (M/r_s)P_s^*/kT_s^* \quad (32)$$

where  $M$  is the solvent molecular weight and  $\rho$  is the experimental bulk solvent density. The pressure may be taken as the solvent saturated vapor pressure (when below the critical point) calculated by equating the S–L chemical potential of the solvent in the bulk liquid and in the vapor. The vapor pressure may also be obtained experimentally.

Combination of eq 21 with the S–L equation of state reveals that the dimensionless CGT temperature  $\Theta/T_s^*$  for an infinite chain is dependent only upon  $r_s$  and the ratio of the polymer and solvent characteristic temperatures defined as  $\xi \equiv T_p^*/T_s^*$ . The behavior of the transition temperature as a function of these parameters is shown in Figure 1. For any given  $r_s$  there will be a critical value  $\xi_c$  at which the transition will occur at the liquid–vapor critical point of the solvent. On the basis of the S–L equations for critical temperature and density of the solvent, this value can be shown to be  $\xi_c = \sqrt{r_s}/(1 + \sqrt{r_s})$ , so

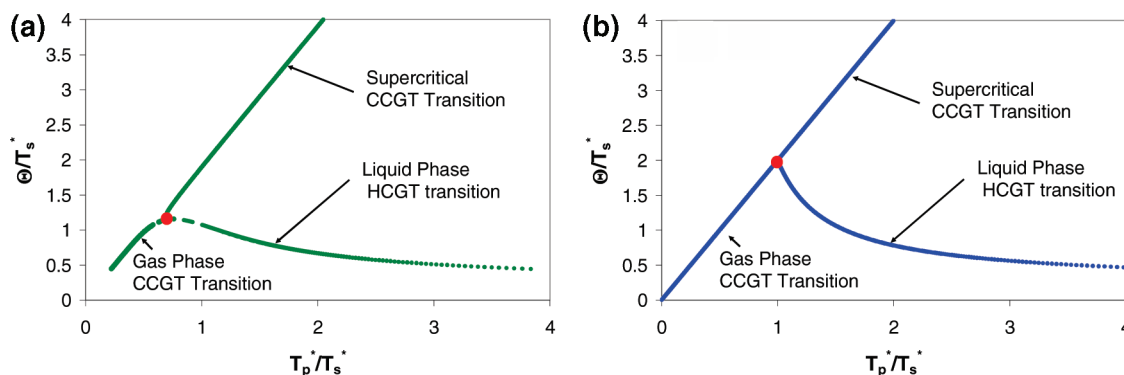


**Figure 1.** Quantitative plot of dimensionless transition temperature vs the ratio of the S–L characteristic temperatures of the polymer and solvent for infinite chain length. (b) is for infinite  $r_s$  while (a) is for  $r_s$  equal to 10. The point marked in red on each plot is the liquid–vapor critical point of the solvent. Each branch from the critical point corresponds to a coil–globule transition for a chain in a different solvent phase, as labeled on the plots. Note that in the limit of infinite  $r_s$  (b) both the gas and supercritical phases are at zero solvent density. Subcritical data are at the solvent saturated vapor pressure while supercritical data are at the solvent critical pressure.

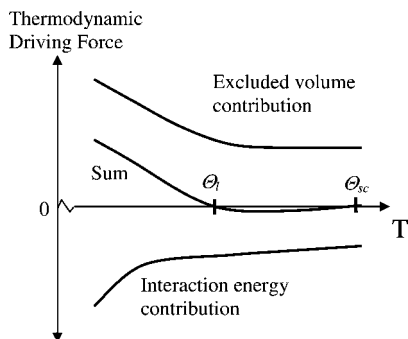


**Figure 2.** Qualitative contributions by excluded volume and polymer self-interaction energy to the rhs of eq 29 as a function of temperature for a system in which the ratio of polymer to solvent S–L characteristic temperature  $\zeta$  is greater than its critical value  $\zeta_c$ . Coil–globule transitions occur when the sum of these contributions is zero.

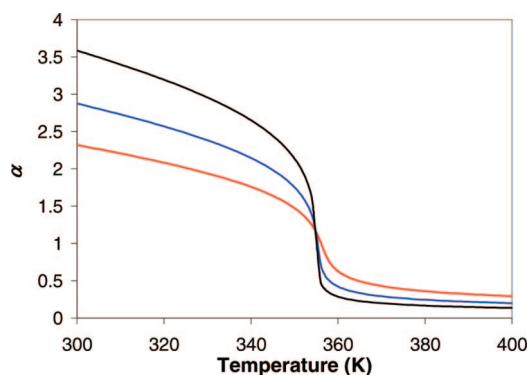


**Figure 3.** Expansion factor as a function of temperature for various molecular weights of polyisobutylene in *n*-pentane near the HCGT. The red line corresponds to a molecular weight of  $10^6$ , the blue to a molecular weight of  $10^7$ , and the black to a molecular weight of  $10^8$ .

that it goes to one as  $r_s$  goes to infinity and one-half as  $r_s$  approaches unity. For  $\zeta < \zeta_c$ , the only transition predicted is a CCGT at  $\Theta_g$  for chains dispersed in the solvent gas phase. For  $\zeta > \zeta_c$ , there will be two physical solutions: an HCGT at  $\Theta_l$  for a chain in the liquid phase solvent and a CCGT at  $\Theta_{sc}$  for a chain at higher temperature in a supercritical solvent.

The predicted transitions can best be understood physically by examining eq 29, which has a straightforward interpretation. The lhs is the chain elastic force that is balanced at equilibrium by the thermodynamic driving forces on the rhs. The rhs is the sum of two terms: a negative term corresponding to the attractive energy of the chain with itself and a positive term corresponding

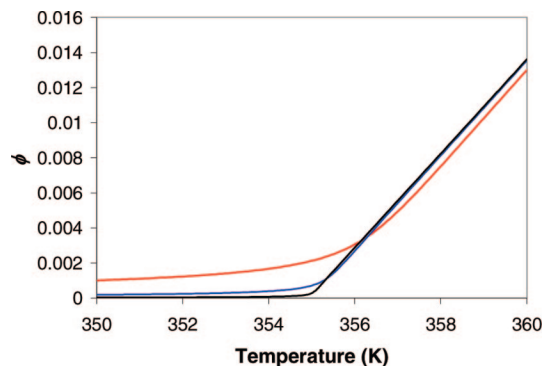


**Figure 4.** Mer density as a function of temperature for various molecular weights of polyisobutylene in *n*-pentane near the HCGT. The red line corresponds to a molecular weight of  $10^6$ , the blue to a molecular weight of  $10^7$ , and the black to a molecular weight of  $10^8$ .

to the excluded volume interaction of the chain with itself and with solvent. The self-interaction energy term always favors chain collapse, while the excluded volume term always favors chain expansion. Equivalently, a positive net driving force corresponds to an expanded coil, a negative net driving force to a collapsed globule, and a zero net driving force to a coil–globule transition. The qualitative contributions of these two thermodynamic forces are shown in Figure 2 for a system with  $\zeta > \zeta_c$ . Furthermore, the derivative of the net driving force with temperature will be positive at a CCGT and negative at a HCGT. The collapsed states associated with both transitions are characterized by dominance of self-interaction energy over excluded volume. Since the polymer self-interaction effect is the only thermodynamic driving force that favors the globule state, this model predicts that a chain with no attractive self-interactions will have no equilibrium globule state. This represents a limitation of this model that is also characteristic of the S–L model, which does not predict an LCST in the absence of attractive interactions. In contrast, simulation studies have predicted a CGT in the absence of attractive interactions.<sup>17,19</sup>

Equation 29 can be used to solve for the gyration radius and chain mer density around the HCGT, yielding results such as those shown in Figure 3 and Figure 4 for a polyisobutylene/*n*-pentane system. For this purpose,  $a = (19/27)^{1/3}$  is consistent with ref 1; however, its precise numerical value is not important, and it could be set equal to unity. As expected, the coil state is predicted at temperatures below the transition while the globular state is predicted at temperatures above the transition. Numerical fitting of results shows that  $S \sim r^{1/3}$  in the globule state and  $S \sim r^{3/5}$  in the coil state, as expected. In addition, the chain mer

**Table 1. Comparison of Solution of Eq 21 with an S–L Solvent at Saturated Vapor Pressure to LCST Data for a Variety of Systems<sup>a</sup>**

polyisobutylene/	density $\rho$ , 25 °C (kg/m <sup>3</sup> )	reduced density $\rho/\rho^*$ , 25 °C	LCST, °C		HCGT, °C
			expt	theor	theor
pentanes					
neopentane	585	0.786	<i>b</i>	−40	42
isopentane	614	0.802	54	53	60
<i>n</i> -pentane	619	0.82	75	72	82
cyclopentane	746	0.86	188	157	147
hexanes					
2,2-dimethylbutane	644	0.833	103	7	101
2,3-dimethylbutane	657	0.841	131	64	114
<i>n</i> -hexane	660	0.852	128	99	134
cyclohexane	783	0.868	243	189	168
other					
<i>n</i> -heptane	691	0.864	168	136	163
<i>n</i> -octane	713	0.875	180	162	194
benzene	877	0.882	260	224	198

<sup>a</sup> Chemically similar solvents are ranked by density. Theoretical LCST's are taken from ref 35. <sup>b</sup> Immiscible at 25 °C.



density  $\phi$  is an appropriate order parameter that is bounded between zero and unity. As shown in Figure 4, it would appear that as the chain approaches infinite density there is a discontinuity at the transition in the slope of  $\phi$  but not in  $\phi$  itself. This is consistent with a second-order thermodynamic transition.

Numerical solution of eq 21 yields good correspondence between predicted HCGT temperatures and experimental and S-L LCST temperatures, as shown in Table 1. The transition temperature was also calculated for most systems using eq 7 rather than eq 8 in order to validate the approximation of eq 8. These calculations yielded results quantitatively consistent with those in Table 1. Because the excluded volume contribution  $1/(1 - \bar{\rho})$  always increases with increased solvent density, this model predicts that higher reduced density solvents will tend to yield cooler CCGTs and warmer HCGTs. As shown in Table 1, for a fixed polymer and like solvent character (i.e., pentanes, hexanes) the ordering of HCGT temperatures  $\Theta_l$  corresponds exactly to the ordering of systems by solvent density.

To the authors' knowledge, HCGT data are available for only one organic system at this time, polystyrene/methyl acetate. For a polystyrene molecular weight of about  $2 \times 10^6$  the LCST is reported to be 116 °C,<sup>42</sup> while light scattering measurements<sup>43</sup> indicate an HCGT temperature in the approximate range of 114–124 °C. Results of eq 18 for this system are in reasonable agreement with these experimental values, with a calculated HCGT temperature of 129 °C.

Longer chain length correlates with warmer CCGTs and cooler HCGTs. This can be determined by a simple examination of the leading order correction to the transition temperature for a finite chain. This correction, calculated in eq 22, corresponds to the second-order term in mer density in eq 20. This correction will always increase the excluded volume effect as chain length decreases, pushing the system toward the coil state. Furthermore, the  $r^{-1/2}$  scaling of the correction is consistent with the chain length scaling of the LCST temperature, which to the leading order also scales as  $r^{-1/2}$ .

## Conclusions

This theory semiquantitatively predicts thermally induced (upon heating) polymer coil-to-globule (HCGT) behavior and temperatures without any adjustable parameters. Equation 21 can be used to calculate the HCGT temperature of a long chain polymer in solvent given only pure component data for the polymer and any empirical or theoretical equation relating density to temperature for the solvent. In most cases these equations provide a good match with experimental lower critical solution transition (LCST) temperatures and with experimental HCGT temperatures, where available. For a solvent density given by the S-L equation of state, systems with an interaction energy ratio  $\xi < \xi_c = \sqrt{r_s}/(1 + \sqrt{r_s})$ , this theory predicts a single CGT which will be a CCGT in the solvent gas phase. For systems with  $\xi > \xi_c$  it predicts two CGTs: an HCGT in the solvent liquid phase and a CCGT in the solvent supercritical phase.

The collapsed states associated with both transitions are characterized by dominance of polymer self-interaction energy over excluded volume effects. Furthermore, higher reduced solvent density correlates with warmer HCGTs and cooler CCGTs due to an increased excluded volume effect. Conversely, longer chain length correlates with cooler HCGTs and warmer CCGTs due to a reduced excluded volume effect.

This model can be easily generalized to treat cross-linked gels and their contraction–expansion characteristics. A coming extension of this model to include electrostatic interactions will address the behavior of polyelectrolytes such as smart synthetic

polymers as well as aspects of DNA and protein behavior such as cold denaturation of proteins.

## References and Notes

- (1) Sanchez, I. C. *Macromolecules* **1979**, *12* (5), 980–988.
- (2) Erman, B.; Flory, P. J. *Macromolecules* **1986**, *19* (9), 2342–2353.
- (3) Grosberg, A. Y.; Kuznetsov, D. V. *Macromolecules* **1992**, *25* (7), 1970–1979.
- (4) Tanaka, G.; Mattice, W. L. *Macromolecules* **1995**, *28* (4), 1049–1059.
- (5) Muthukumar, M. J. *Chem. Phys.* **1984**, *81* (12), 6272–6276.
- (6) Yamakawa, H. *Macromolecules* **1993**, *26* (19), 5061–5066.
- (7) Nakata, M. *Phys. Rev. E* **1995**, *51* (6), 5770–5775.
- (8) Nakata, M.; Nakagawa, T. *Phys. Rev. E* **1997**, *56* (3), 3338–3345.
- (9) Hamurcu, E. E.; Akcelrud, L.; Baysal, B. M.; Karasz, F. E. *Polymer* **1998**, *39* (16), 3657–3663.
- (10) Nakata, M.; Nakagawa, T. *J. Chem. Phys.* **1999**, *110* (5), 2703–2710.
- (11) Nakamura, Y.; Sasaki, N.; Nakata, M. *Macromolecules* **2001**, *34* (17), 5992–6002.
- (12) Zhang, G.; Wu, C. J. *Am. Chem. Soc.* **2001**, *123* (7), 1376–1380.
- (13) Dogan, M.; Kuntman, A. *Polym. Int.* **2000**, *49* (12), 1648–1652.
- (14) Gurel, E. E.; Kayaman, N.; Baysal, B. M.; Karasz, F. E. *J. Polym. Sci., Part B: Polym. Phys.* **1999**, *37* (16), 2253–2260.
- (15) Polson, J. M.; Moore, N. E. *J. Chem. Phys.* **2005**, *122* (2), 0249051–02490511.
- (16) Szeleifer, I.; Otoole, E. M.; Panagiotopoulos, A. Z. *J. Chem. Phys.* **1992**, *97* (9), 6802–6808.
- (17) Dijkstra, M.; Frenkel, D.; Hansen, J. P. *J. Chem. Phys.* **1994**, *101* (4), 3179–3189.
- (18) Dijkstra, M.; Frenkel, D. *Phys. Rev. E* **1994**, *50* (1), 349–357.
- (19) Luna-Barcenas, G.; Bennett, G. E.; Sanchez, I. C.; Johnston, K. P. *J. Chem. Phys.* **1996**, *104* (24), 9971–9973.
- (20) Luna-Barcenas, G.; Gromov, D. G.; Meredith, J. C.; Sanchez, I. C.; dePablo, J. J.; Johnston, K. P. *Chem. Phys. Lett.* **1997**, *278* (4–6), 302–306.
- (21) Luna-Barcenas, G.; Meredith, J. C.; Sanchez, I. C.; Johnston, K. P.; Gromov, D. G.; de Pablo, J. J. *J. Chem. Phys.* **1997**, *107* (24), 10782–10792.
- (22) Khalatur, P. G.; Zherenkova, L. V.; Khokhlov, A. R. *Eur. Phys. J. B* **1998**, *5* (4), 881–897.
- (23) Lang, D. *J. Mol. Biol.* **1973**, *78*.
- (24) Lang, D.; Taylor, T. N.; Dobyan, D. C.; Gray, D. M. *J. Mol. Biol.* **1976**, *106* (1), 97–107.
- (25) Vasilevskaya, V. V.; Khokhlov, A. R.; Matsuzawa, Y.; Yoshikawa, K. *J. Chem. Phys.* **1995**, *102* (16), 6595–6602.
- (26) Melnikov, S. M.; Sergeyev, V. G.; Yoshikawa, K. *J. Am. Chem. Soc.* **1995**, *117* (40), 9951–9956.
- (27) Dias, R. S.; Innerlohinger, J.; Glatter, O.; Miguel, M. G.; Lindman, B. *J. Phys. Chem. B* **2005**, *109* (20), 10458–10463.
- (28) Sherman, E.; Haran, G. *Proc. Natl. Acad. Sci. U.S.A.* **2006**, *103* (31), 11539–11543.
- (29) Sadqi, M.; Lapidus, L. J.; Munoz, V. *Proc. Natl. Acad. Sci. U.S.A.* **2003**, *100* (21), 12117–12122.
- (30) Pollack, L.; Tate, M. W.; Finnefrock, A. C.; Kalidas, C.; Trotter, S.; Darnton, N. C.; Lurio, L.; Austin, R. H.; Batt, C. A.; Gruner, S. M.; Mochrie, S. G. *J. Phys. Rev. Lett.* **2001**, *86* (21), 4962–4965.
- (31) Welker, E.; Maki, K.; Shastry, M. C. R.; Juminaga, D.; Bhat, R.; Scheraga, H. A.; Roder, H. *Proc. Natl. Acad. Sci. U.S.A.* **2004**, *101* (51), 17681–17686.
- (32) Urry, D. W. *J. Phys. Chem. B* **1997**, *101* (51), 11007–11028.
- (33) Kubota, K.; Fujishige, S. *J. Phys. Chem.* **1990**, *94*, 5154–5158.
- (34) Gao, J.; Wu, C. *Macromolecules* **1997**, *30*, 6873–6876.
- (35) Xhang, X. Z.; Zhou, R. X.; Cui, J. Z.; Zhang, J. T. *Int. J. Pharm.* **2002**, *235*, 43–50.
- (36) Joeong, B.; Kim, S. W.; Bae, Y. H. *Adv. Drug Delivery Rev.* **2002**, *54*, 37–51.
- (37) Ballauff, M.; Lu, Y. *Polymer* **2007**, *48*, 1815–1823.
- (38) Lowe, C. P.; Dreischor, M. W. *J. Chem. Phys.* **2005**, *122* (8), 0849051–0849057.
- (39) Lacombe, R. H.; Sanchez, I. C. *J. Phys. Chem.* **1976**, *80* (23), 2569–2580.
- (40) Flory, P. J.; Fisk, S. J. *Chem. Phys.* **1966**, *44*.
- (41) Sanchez, I. C.; Stone, M. In *Polymer Blends*; Paul, D. R., Bucknall, C. B., Eds.; John Wiley & Sons: New York, 2000; Vol. 1, p 51.
- (42) Saeki, S.; Konno, S.; Kuwahara, N.; Nakata, M.; Kaneko, M. *Macromolecules* **1974**, *7* (4), 521–526.
- (43) Chu, B.; Park, I. H.; Wang, Q. W.; Wu, C. *Macromolecules* **1987**, *20* (11), 2833–2840.